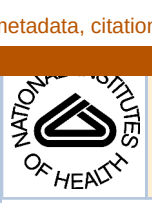

Published in final edited form as:

ACS Chem Biol. 2008 August 15; 3(8): 480–485. doi:10.1021/cb800069c.

mRNA Display Selection of a High-Affinity, Modification-Specific Phospho-IκBα-Binding Fibronectin

C. Anders Olson[†], **Hsiang-I Liao**[§], **Ren Sun**[§], and **Richard W. Roberts**[‡,*]

[†]Biochemistry and Molecular Biophysics Option, California Institute of Technology, Pasadena, California 91125

[‡]Departments of Chemistry, Chemical Engineering/Materials Science, and Biology, University of Southern California, Los Angeles, California 90089-1211

[§]Department of Molecular and Medical Pharmacology, University of California, Los Angeles, California 90095

Abstract

The complexity of the human proteome is greatly expanded by post-translational modifications. New tools capable of recognizing these modifications in a sequence-specific fashion provide a route to purify these modified proteins, to alter protein trafficking, and to visualize signal transduction in real time. Here, we have evolved novel, modification-specific ligands that target phosphorylated IκBα. To do this, we employed mRNA display-based *in vitro* selection using a 30-trillion-member protein library based on the fibronectin type III domain. The selection yielded one fibronectin molecule, 10C17C25, that binds a phospho-IκBα peptide with K_d = 18 nM and is over 1000-fold specific compared to the nonphosphorylated peptide. 10C17C25 specifically recognizes endogenous phosphorylated IκBα from mammalian cell extract and stabilizes phospho-IκBα *in vivo*. We also incorporated 10C17C25 into a FRET indicator that detects IκB kinase (IKK) activity *in vitro*, demonstrating the utility of selecting designed adaptors for kinase activity sensors.

Whereas the human genome contains less than 25,000 genes, the proteome likely contains over 1,000,000 different proteins when alternative splicing and post-translational modifications (PTM) are taken into account (1). Post-translational modifications are essential to cellular signaling, and the ability to detect and quantitate modifications is challenging but immensely valuable. Nucleic-acid-based microarrays are powerful proteomic tools, although they cannot detect the presence and extent of PTMs and may not be accurate predictors of protein quantities (2). Attempts to generate open-access resources for modification-specific affinity reagents to all proteins are currently under way (3). In addition to detection *in vitro*, novel protein affinity reagents that are functional in the intracellular environment are also useful for determining protein localization and for assessing protein function (4,5). Compared to gene and transcript knockout techniques, domain and state-specific protein binders that knock down activity may be better determinants of protein function (6). Increasingly, *in vitro* selection techniques such as ribosome display and mRNA display are being implemented to generate novel protein-based affinity reagents with alternative scaffolds (7–9). Nonimmunoglobulin scaffolds such as the ankyrin-based “DARPins” (10) and fibronectin type III “monobodies” (11) have advantages over antibodies for both *in vitro* and *in vivo* applications because they (i) lack disulfide bonds, (ii) can be expressed efficiently in bacteria and eukaryotic cells, and (iii) possess improved stability (12).

*Corresponding author, richrob@usc.edu.

Supporting Information *Available*: This material is free of charge *via* the Internet.

Intrinsically unstructured domains compose a large fraction of the proteome, and many are subjected to PTM (1,13). An example of such a domain is the N-terminus of IκB. In the classical NF-κB pathway, three IκB proteins, IκBα, β, and ∈, regulate the activity of the ubiquitous transcription factor NF-κB (14). NF-κB plays an important role in inflammation and is implicated in autoimmune disease and cancer (15). Upon stimulation, IκB kinase (IKK) immediately phosphorylates IκBα at serines 32 and 36 (16,17). IκBα is then ubiquitinated by the SCF-βTrCP E3 ligase complex and degraded by the proteasome, thereby freeing NF-κB to direct transcription (18). Reagents that detect or inhibit the degradation of IκBα *in vivo* may be useful in order to understand the many complex pathways to NF-κB activation. Inhibition at this control point is ideal since the functions of IKK and βTrCP are not specific to the classical NF-κB pathway (15,19).

We employed *in vitro* selection by mRNA display to generate novel protein affinity reagents that recognize phosphorylated IκBα specifically. We utilized a combinatorial protein library based on the 10th fibronectin type III domain of human fibronectin (10FnIII) to generate protein molecules that are functional both *in vitro* and *in vivo* (20). The target used for this selection was a synthetic phospho-peptide corresponding to amino acid residues 22–41 of human IκBα. This peptide contains the E3 ligase recognition sequence including phosphorylated serines 32 and 36, which are essential for degradation. The target peptide contained an N-terminal biotin spaced by aminohexanoic acid for specific immobilization to either neutravidin agarose or streptavidin acrylamide beads.

The first round of selection was carried out so that the first affinity enrichment step contained at least three copies of the 30-trillion-member 10FnIII library (21). Enrichment was monitored by measuring radiolabeled fusion binding (Figure 1, panel a). In order to reduce the enrichment of bead binders, a negative selection step was employed at round 6. After 10 rounds of selection, pool 10 was determined to have approximately 50% binding efficiency at RT with relatively low background binding (1%). Figure 1 (panel b) demonstrates that pool 10 binding is both sequence-specific and phospho-specific. Binding to a nonphosphorylated IκBα peptide otherwise identical to the target was equal to background. Likewise, phospho-serines alone are not sufficient for binding. No binding was detected above background to a peptide corresponding to Elk1 residues 380–394 containing two phosphorylated serines.

Pool 10 was cloned, and 11 sequences were obtained. All 11 sequences were highly similar, suggesting that all sequences share a common ancestor (see Supporting Information). One representative sequence, 10C17, is illustrated in Figure 2, panel a. The wild-type sequence shown represents a 7-residue deletion mutant previously described as 10FnIII (Δ1–7) and has equivalent expression, solubility, and folding stability as full-length 10FnIII (20). Essentially, only one solution to the molecular recognition of phospho-IκBα was obtained. This may be due to an intrinsic rarity of binders in the library, as obtaining binders to non-structured targets may be more difficult than obtaining binders to structured targets. Alternatively, it is possible that the pool reached an artificial bottleneck due to overly stringent selection conditions or that the immobilization scheme on streptavidin beads limited accessibility of the target.

The ability for the binders to express in bacteria is important for their utility as affinity reagents. Both 10C17 and another pool 10 clone, 10C19, do not express well in *E. coli* BL21(DE3) (data not shown). In order to improve the expression of 10C17, solubility was evolved using the GFP reporter screen developed by Waldo *et al.* (22). Three rounds of evolution (A, B, and C) were performed using error-prone PCR so that one or two mutations were generated per gene. Representative sequences obtained from each of the three rounds of evolution performed are listed in Figure 2, panel a. Approximately 2000 colonies were screened in each round, and the brightest 24 colonies were picked and assayed. The improvement in expression was analyzed by comparing total cell fluorescence of 10C17-GFP variants relative to that of WT 10FnIII

(Figure 2, panel b). For the first two rounds of evolution, expression was induced with IPTG for 4 h (screen 1). We found that although the initial mutations improved expression, the result of the long induction was that fluorescent aggregates were able to accumulate. This resulted in obtaining variants that performed better than wild-type (WT) 10FnIII in the assay but did not express as well. We found that decreasing the length of expression to 1.5 h improved the sensitivity of the screen (Figure 2, panel b, screen 2). In order to ensure that function was retained, binding was measured for each of the variants using SDS-PAGE quantitated by autoradiography (Figure 2, panel c).

From round one of the evolution, one variant containing two mutations was obtained (A21) that improved both solubility and binding (Figure 2). Two sequences were obtained from round two that improved solubility and did not affect binding. B11 was a unique clone, whereas the B01 sequence was found three times out of the 24 clones assayed. We created 10C17B25 by combining the two beneficial point mutations selected, L13Q and A10T, from B11 and B01, respectively. 10C17B25 displays an additive improvement in solubility. The third round of evolution again generated two variants both with improved expression (C21, which was found twice, and C22, which was unique). The two mutations selected in C21 and C22 were combined to produce 10C17C25, which binds with approximately 94% efficiency (Figure 2, panels a and c). This variant could be expressed at modest levels in bacteria (1 mg L^{-1} culture) and was purified by nickel affinity and ion exchange chromatography.

The fact that we obtained improvements in both solubility and binding argues that the mutations increased the overall stability of the domain. Of the six mutations we implemented to obtain the 10C17C25 variant, only four positions differ from WT 10FnIII. Two mutations were obtained at position Val6 (originally Ala in WT 10FnIII), V6D and D6E. Also, Ala10 reverted back to Thr, the wild-type residue (Figure 2, panel a). Mutations V6E and L13Q are notable because they are both likely solvent-exposed and close in space (Figure 2, panel d) (23). At these two positions, the mutations altered what had been a large hydrophobic patch on the protein surface, making it more polar with residues that have the potential to interact favorably. In addition to these positive mutations, we also found changes that improved solubility but negatively affected function (for example, variants B16 and C18, which were found three and six times out of 24 clones in pools B and C, respectively).

We next addressed the affinity and specificity of 10C17C25, as well as its ability to bind endogenous phospho-IκBα from human cell culture (Figure 3). 10C17C25 was subcloned into a modified pET 21 vector that generates a C-terminal MBP fusion with a C-terminal His-tag. MBP was used to increase the expression of 10C17C25 (45 mg L^{-1} culture) and provide an additional affinity purification tag. Binding to both the phosphorylated and nonphosphorylated IκBα peptides was measured using a Biacore T100 instrument (Figure 3, panels a and b). 10C17C25-MBP binds phospho-IκBα with K_d = 18 nM, which is comparable to high-affinity antibodies (24). Binding to the nonphosphorylated peptide was not detected at the highest concentration of 10C17C25-MBP tested (28 μM) (Figure 3, panel b). Therefore, the specificity of 10C17C25 for the phosphorylated state is >1000-fold.

We next wanted to determine whether 10C17C25 is able to recognize wild-type, full-length IκBα specifically in its phosphorylated state. Phospho-IκBα was produced in 293T cells by stimulation with TNF-α and was stabilized by addition of the protease inhibitor calyculin A and the proteasome inhibitor MG132. Both stimulated and unstimulated cells were lysed with Tris-buffered saline plus 1% triton x-100. 10C17C25-MBP was added to the cleared lysates and incubated with nickel-NTA beads. A Western blot performed to detect the presence of IκBα using a polyclonal antibody demonstrates that 10C17C25 is able to bind full-length IκBα only from TNF-α stimulated cells (Figure 3, panel c). IκBα that is immobilized by 10C17C25 has a noticeable reduction in mobility typical of phosphorylated IκBα (16).

We also tested the ability of 10C17C25 to express and function in human cells. 10C17C25 was cloned into a modified pIRES-puro vector containing a C-terminal GFP. This fusion protein was well-expressed throughout the cytoplasm and nucleus of 293T cells when transiently transfected. 10C17C25-GFP is able to stabilize phospho-IκBα *in vivo* when transiently expressed (Figure 3, panel d). Expression of 10C17C25-GFP stabilizes phospho-IκBα even after 30 min of TNF-α incubation, when IκBα degradation is maximal in 293T cells. Phospho-IκBα is not detected in cells expressing Fn04, a nonselected fibronectin control, as phospho-IκBα is rapidly degraded without an inhibitor present (Figure 3, panel d).

FRET sensors have been employed to detect PTMs reversibly *in vivo* in a spatial and temporal manner (25–27). The sensors previously developed utilize natural modification-specific binding domains such as SH2 and a chromodomain. These sensors contain an enzyme substrate sequence that is bound by the proximal binding domain upon modification when signaling is active. This binding restrains the sensor, resulting in a change in FRET between an N-terminal CFP and a C-terminal YFP. The potential for such sensors can be greatly expanded by applying *in vitro* selection to create novel modification-specific binding domains. We demonstrated this by creating a FRET-based sensor for IKK activity and assessed its function *in vitro* (Figure 4, panel a). CFP, YFP, and a new multiple cloning site that contains a flexible linker sequence were cloned into a pET21 $(His)_6$-tag vector (see Supporting Information). 10C17C25 and a Klenow extended fragment encoding IκBα residues 23–41 were cloned into the vector in two orientations with short and long linkers (Figure 4, panel b). The second orientation (IKK FS C25 2S and 2L) contains longer linkers than the first (IKK FS C25 1S and 1L) due to the location of the binding surface relative to the termini of the fibronectin domain. A nonselected fibronectin variant was also cloned into one orientation as a control (IKK FS Fn04 control).

The five constructs were expressed in *E. coli* BL21(DE3) and purified by nickel-NTA affinity chromatography. The constructs were phosphorylated *in vitro* with recombinant IKK-β, and the reactions were terminated by addition of EDTA after 1 h. FRET was then measured on constructs with or without incubation with IKK-β (Figure 4, panel c). FRET was quantitated by measuring the ratio of the YFP emission intensity and the CFP emission intensity after excitation at $\lambda = 435$ nm and is represented as a percent change after incubation with kinase (Figure 4, panel b). The first orientation results in a small decrease in FRET after IKK-β incubation, whereas the second orientation results in a substantial increase in FRET. The length of the linker does not significantly affect the change in FRET, and phosphorylation of the control sensor does not result in a change in FRET. This indicates that neither phosphorylation alone nor interaction with IKK-β can account for the changes in FRET observed with IKK FS C25 2S and 2L. Likewise, the FRET response is demonstrated to be a result of binding to the phosphorylated IκBα sequence as excess phospho-peptide reduces the FRET response achieved after incubation with kinase (Figure 4, panel c). Western blot was performed using a monoclonal phospho(S32/S36)-specific anti-IκBα antibody to demonstrate that the kinase reaction is efficient and phosphorylation does occur (Figure 4, panel d).

In conclusion, we have demonstrated the utility of mRNA display using a combinatorial protein library based on the 10FnIII scaffold for modification-specific recognition of protein domains. We have demonstrated that the selection, combined with solubility evolution, was able to produce a high-affinity, high-specificity binder to phospho-IκBα. This scaffolded library is ideally suited to discrimination of modifications due to the flexible, continuous ligand binding surface generated by the randomized loops (20). We have also demonstrated utility of the library for binding unstructured epitopes with high affinity. 10C17C25 has been demonstrated to not only recognize phospho-IκBα *in vitro* but also to bind and inhibit degradation *in vivo*. This intracellular inhibition may prove useful for studying the complex NF-κB pathway as an alternative to gene knockout or overexpression of modified IκB.

Methods

Reagents

Oligonucleotides were synthesized by IDT or the Yale Keck oligonucleotide synthesis facility. Oligonucleotide sequences are listed in Supporting Information. Peptides were synthesized by Biomer-Tech and purified by reverse-phase HPLC. Products were confirmed by electrospray mass spectrometry. For plasmid construction and cloning, see Supporting Information. *E. coli* BL21(DE3) was purchased from Novagen. 293T cells were cultured in Dulbecco's modified Eagle's medium plus 10% fetal bovine serum (Invitrogen).

Selection

The library used in this selection was previously described (20). Protein-mRNA fusions were generated as previously described (21). Briefly, each round of selection includes PCR, *in vitro* transcription, splint mediated ligation to a 3′ puromycin-containing DNA linker (T4 DNA ligase, NEB), urea PAGE purification, reticulocyte lysate translation (Red Nova, Novagen), salt-induced fusion formation, oligo-dT cellulose purification (NEB), reverse transcription (Superscript II, Invitrogen), and affinity enrichment. For the first round of selection, the 30-trillion-member library was generated with at least three copies of fusions. Affinity enrichment was typically performed with 10–20 μL of beads saturated with peptide (neutravidin agarose or streptavidin ultralink beads, Pierce). The selection buffer included PBS supplemented with 0.5 mg mL^{-1} BSA (Sigma), 0.1 mg mL^{-1} sheared salmon sperm DNA (Sigma), 0.02% Tween 20, and 1 mM DTT. A negative selection step was performed beginning at round 6 following reverse transcription by flowing fusions over ~100 μL of empty blocked beads in column format. Free neutravidin or streptavidin (Pierce) was also including in the selection binding buffer to compete with background binders. Binding was measured by scintillation counting of ^{35}S-methionine labeled, oligo-dT cellulose purified fusions. All radiolabeled binding assays were performed at RT. Pool 10 was cloned into a TOPO-TA vector (Invitrogen) for sequencing.

Solubility Evolution

Error-prone PCR was performed with 7 mM $MgCl_2$ and 0.05 mM $MnCl_2$ to generate one or two mutations per gene. The GFP reporter screen and fluorescence quantitation was carried out as previously described (20,22). In each round, 24 colonies were picked and assayed prior to sequencing. In some cases, three or more identical clones had been picked, and these independent experiments led to standard deviations of 4.1%, 4.0%, and 3.3% for B01, B16, and C18, respectively. To test retention of function, crude ^{35}S-Methionine labeled, *in vitro* translated protein was bound to immobilized target peptide or empty beads, washed, and eluted with SDS PAGE loading buffer. An equivalent amount of crude translation product, and eluted protein was analyzed by SDS-PAGE autoradiography to determine percent protein bound.

Surface Plasmon Resonance

SPR was performed on a Biacore T100 instrument (USC NanoBiophysics Core Facility). 10C17C25-MBP was expressed in *E. coli* BL21(DE3) by induction with 1 mM IPTG at mid-log phase for 3 h. Pelleted cells were lysed with B-PER (Pierce) and affinity-purified with a nickel-NTA column (Qiagen), followed by affinity purification with an amylose resin column (NEB) and desalting (PD-10, Amersham Biosciences). Biacore buffer included PBS plus 0.5 mg mL^{-1} BSA and 0.05% Tween 20. Various concentrations of analyte were flowed at 100 μL/min for 2 min at RT and allowed to dissociate for 45 min. Binding sensograms were fitted with Biacore evaluation software.

Pull-Down

Confluent 293T cell culture was incubated with TNF-α (20 ng mL^{-1}), MG132 (10 μM), and calyculin A (50 nM), respectively, for 15 min (Calbiochem). Stimulated and unstimulated cells were lysed for 5 min with ice-cold lysis buffer (PBS, 1% triton x-100, 20 ng mL^{-1} MG132, 100 nM calyculin A, protease inhibitor cocktail III (Calbiochem), and 1 mM EDTA). MG132 was required during lysis and binding to prevent degradation and depletion of phosphorylated IκBα. Cell extracts were cleared by centrifugation at 20,000*g* for 5 min, combined with purified 10C17C25-MBP, and incubated with nickel-NTA beads for 1 h at 4 °C. After three washes, samples were eluted with PAGE loading buffer. Crude cell extracts from stimulated and unstimulated cells were run with the eluted samples on SDS-PAGE (NuPAGE system, Invitrogen), transferred to PVDF membrane (Biorad), and incubated with polyclonal anti-IκBα (C21) antibody (Santa Cruz Biotechnology). After secondary antibody incubation, blots were incubated with SuperSignal West Dura substrate (Pierce) and imaged by chemiluminescence with an Alpha Imager equipped with a cooled CCD camera.

In Vivo Inhibition

293T cells were transiently transfected with 10C17C25-GFP or Fn04-GFP using Lipofectamine Plus reagent (Invitrogen) following the manufacturers recommendations. One day post-transfection, cells were stimulated with 20 ng mL^{-1} TNF-α for the indicated time. Crude cell extracts were prepared and analyzed by Western blot.

IKK FRET Sensor

FRET sensor proteins were expressed as described for 10C17C25-MBP. Nickel-NTA affinity purified sensors (50 μg mL^{-1}) were kinased with recombinant IKKβ (1 μg mL^{-1}, Invitrogen) in 20 mM Tris, pH 7.5 plus 10 mM $MgCl_2$ and 200 μM ATP. Reactions were terminated by addition of EDTA. Fluorescence emission spectra were obtained using a Shimadzu fluorimeter RF-5301PC by excitation at 435 nm with 5 nm slit widths. FRET was calculated as the emission intensity at 525 nm divided by the intensity at 475 nm. Western blot was performed as described using a monoclonal phospho-IκBα (5A5) antibody (Cell signaling Technology).

Supplementary Material

Refer to Web version on PubMed Central for supplementary material.

Acknowledgments

We thank Dr. T. Leung and Dr. M. Boldin (Caltech) for advice. We thank Dr. Geoffrey S. Waldo (Los Alamos National Laboratory) for donation of the GFP reporter vector and Dr. Jose Aberola-Ila (Oklahoma Medical Research Foundation) for donation of ECFP and EYFP plasmids. C.A.O. was supported by an NSF graduate fellowship. Funding was provided by NIH RO1 GM60416 (R.W.R.), and the American Foundation for AIDS Research (R.W.R.).

References

1. Jensen ON. Modification-specific proteomics: characterization of post-translational modifications by mass spectrometry. Curr Opin Chem Biol 2004;8:33–41. [PubMed: 15036154]
2. Gygi SP, Rochon Y, Franza BR, Aebersold R. Correlation between protein and mRNA abundance in yeast. Mol Cell Biol 1999;19:1720–30. [PubMed: 10022859]
3. Taussig MJ, Stoevesandt O, Borrebaeck CA, Bradbury AR, Cahill D, Cambillau C, de Daruvar A, Dubel S, Eichler J, Frank R, Gibson TJ, Gloriam D, Gold L, Herberg FW, Hermjakob H, Hoheisel JD, Joos TO, Kallioniemi O, Koegl M, Konthur Z, Korn B, Kremmer E, Krobitsch S, Landegren U, van der Maarel S, McCafferty J, Muyldermans S, Nygren PA, Palcy S, Pluckthun A, Polic B, Przybylski M, Saviranta P, Sawyer A, Sherman DJ, Skerra A, Templin M, Ueffing M, Uhlen M. ProteomeBinders:

planning a European resource of affinity reagents for analysis of the human proteome. Nat Methods 2007;4:13–7. [PubMed: 17195019]

4. Nizak C, Monier S, del Nery E, Moutel S, Goud B, Perez F. Recombinant antibodies to the small GTPase Rab6 as conformation sensors. Science 2003;300:984–7. [PubMed: 12738866]
5. Carlson JR. A new means of inducibly inactivating a cellular protein. Mol Cell Biol 1988;8:2638–46. [PubMed: 3136320]
6. Stocks M. Intrabodies as drug discovery tools and therapeutics. Curr Opin Chem Biol 2005;9:359–65. [PubMed: 15979379]
7. Lipovsek D, Pluckthun A. In-vitro protein evolution by ribosome display and mRNA display. J Immunol Methods 2004;290:51–67. [PubMed: 15261571]
8. Roberts RW, Szostak JW. RNA-peptide fusions for the in vitro selection of peptides and proteins. Proc Natl Acad Sci USA 1997;94:12297–302. [PubMed: 9356443]
9. Hanes J, Pluckthun A. In vitro selection and evolution of functional proteins by using ribosome display. Proc Natl Acad Sci USA 1997;94:4937–42. [PubMed: 9144168]
10. Kawe M, Forrer P, Amstutz P, Pluckthun A. Isolation of intracellular proteinase inhibitors derived from designed ankyrin repeat proteins by genetic screening. J Biol Chem 2006;281:40252–63. [PubMed: 17050543]
11. Koide A, Abbatiello S, Rothgery L, Koide S. Probing protein conformational changes in living cells by using designer binding proteins: application to the estrogen receptor. Proc Natl Acad Sci USA 2002;99:1253–8. [PubMed: 11818562]
12. Skerra A. Alternative non-antibody scaffolds for molecular recognition. Curr Opin Biotechnol 2007;18:295–304. [PubMed: 17643280]
13. Stoevesandt O, Taussig MJ. Affinity reagent resources for human proteome detection: initiatives and perspectives. Proteomics 2007;7:2738–50. [PubMed: 17639606]
14. Hoffmann A, Levchenko A, Scott ML, Baltimore D. The IκB-NF-κB signaling module: temporal control and selective gene activation. Science 2002;298:1241–5. [PubMed: 12424381]
15. Viatour P, Merville MP, Bours V, Chariot A. Phosphorylation of NF-κB and IκB proteins: implications in cancer and inflammation. Trends Biochem Sci 2005;30:43–52. [PubMed: 15653325]
16. Brown K, Gerstberger S, Carlson L, Franzoso G, Siebenlist U. Control of IκB-α proteolysis by site-specific, signal-induced phosphorylation. Science 1995;267:1485–8. [PubMed: 7878466]
17. DiDonato JA, Hayakawa M, Rothwarf DM, Zandi E, Karin M. A cytokine-responsive IκB kinase that activates the transcription factor NF-κB. Nature 1997;388:548–54. [PubMed: 9252186]
18. Yaron A, Hatzubai A, Davis M, Lavon I, Amit S, Manning AM, Andersen JS, Mann M, Mercurio F, Ben-Neriah Y. Identification of the receptor component of the IκBα-ubiquitin ligase. Nature 1998;396:590–4. [PubMed: 9859996]
19. Fuchs SY, Spiegelman VS, Kumar KG. The many faces of beta-TrCP E3 ubiquitin ligases: reflections in the magic mirror of cancer. Oncogene 2004;23:36. 2028.
20. Olson CA, Roberts RW. Design, expression, and stability of a diverse protein library based on the human fibronectin type III domain. Protein Sci 2007;16:476–84. [PubMed: 17322532]
21. Liu R, Barrick JE, Szostak JW, Roberts RW. Optimized synthesis of RNA-protein fusions for in vitro protein selection. Methods Enzymol 2000;318:268–93. [PubMed: 10889994]
22. Waldo GS, Standish BM, Berendzen J, Terwilliger TC. Rapid protein-folding assay using green fluorescent protein. Nat Biotechnol 1999;17:691–5. [PubMed: 10404163]
23. Leahy DJ, Aukhil I, Erickson HP. 2.0 A crystal structure of a four-domain segment of human fibronectin encompassing the RGD loop and synergy region. Cell 1996;84:155–64. [PubMed: 8548820]
24. Carter PJ. Potent antibody therapeutics by design. Nat Rev Immunol 2006;6:343–57. [PubMed: 16622479]
25. Lin CW, Jao CY, Ting AY. Genetically encoded fluorescent reporters of histone methylation in living cells. J Am Chem Soc 2004;126:5982–3. [PubMed: 15137760]
26. Sato M, Ozawa T, Inukai K, Asano T, Umezawa Y. Fluorescent indicators for imaging protein phosphorylation in single living cells. Nat Biotechnol 2002;20:287–94. [PubMed: 11875431]

27. Wang Y, Botvinick EL, Zhao Y, Berns MW, Usami S, Tsien RY, Chien S. Visualizing the mechanical activation of Src. Nature 2005;434:1040–5. [PubMed: 15846350]

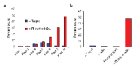

Figure 1.
Selection of phospho-IκBα binders. a) Enrichment of target binders was monitored by radiolabeled fusion binding assays. b) Pool 10 binding is sequence-specific and phospho-specific.

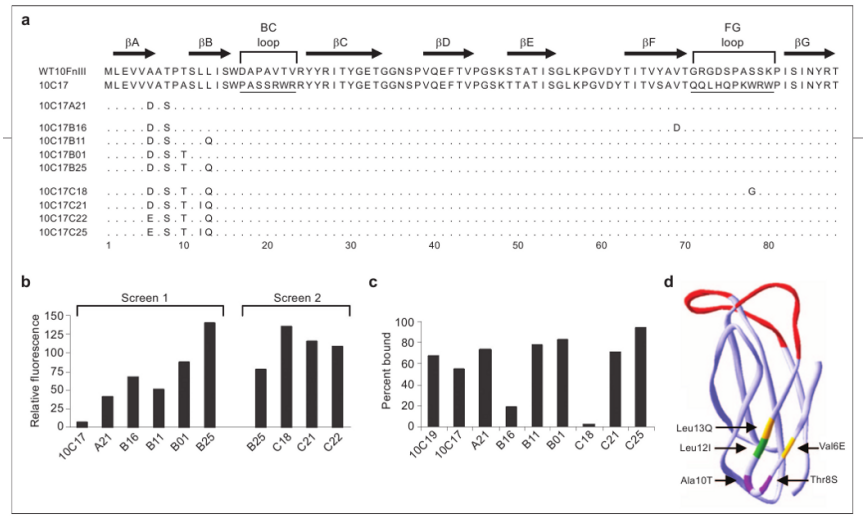

Figure 2.

Solubility evolution of selection winner using a GFP reporter screen (22). a) Sequence of wild-type 10FnIII, a pool 10 clone (10C17), and evolved variants of 10C17 from three rounds of evolution. Dots represent sequence identical to 10C17. b) Total cell fluorescence of expression cultures relative to wild-type 10FnIII. Proteins were expressed for 4 h (screen 1) or 1.5 h (screen 2). c) Binding of selected clones with *in vitro* translated protein measured by SDS-PAGE autoradiography (representative data). d) Locations of evolved mutations on the 10FnIII surface include solvent-exposed (yellow), buried (green), and AB loop (purple).

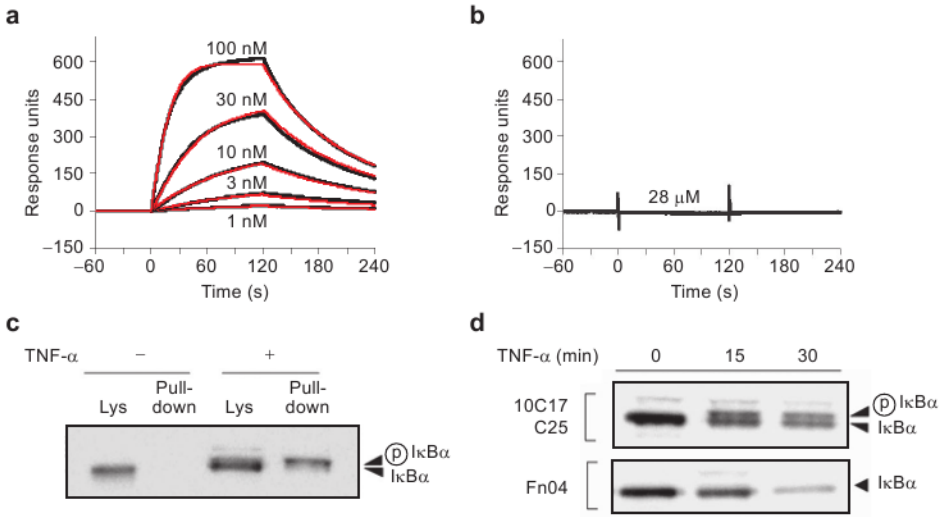

Figure 3.

Affinity and specificity of 10C17C25. SPR was performed to test affinity and specificity to phospho-IκBα. Concentrations of 10C17C25-MBP ranged from 1–100 nM for phospho-IκBα binding (panel a) and up to 28 μM for nonphosphorylated IκBα peptide binding (panel b). Black represents raw data, red represents curve fits. c) Modification-specific binding to full-length IκBα was determined by pull-down from mammalian cell culture. d) Intracellular function was demonstrated by the inhibition of IκBα degradation in TNF-α stimulated 293T cells transiently transfected with 10C17C25-GFP. Cells transiently transfected with nonselected Fn04-GFP were used as a control.

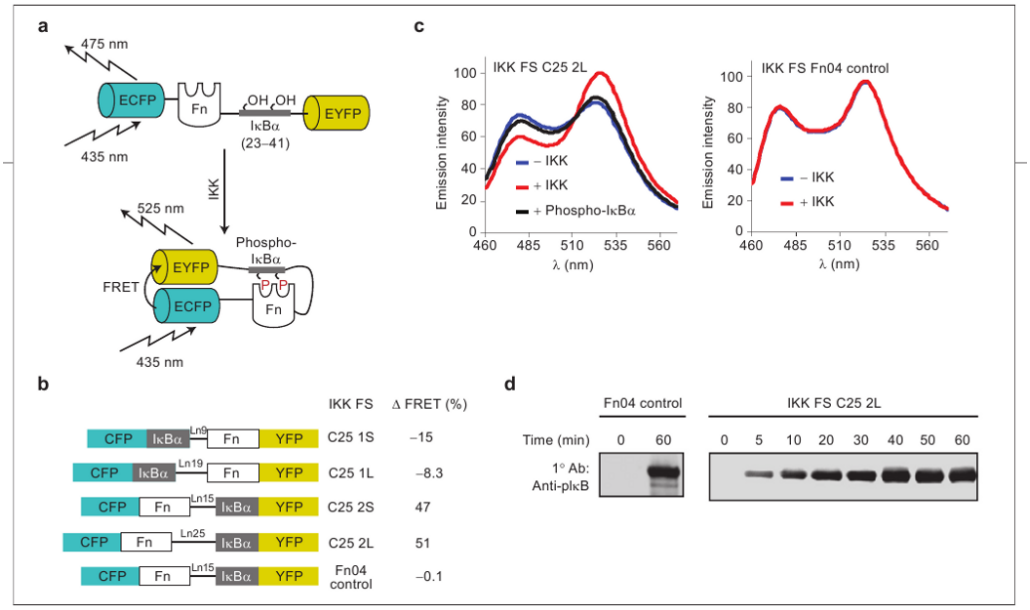

Figure 4.

IKK FRET sensor. a) Illustration of a FRET sensor for IKK activity using a designed modification-specific fibronectin (Fn) binder. b) Four sensors were created, as well as a control containing nonselected Fn04. The IKK substrate sequence corresponds to IκBα residues 23–41. c) Representative fluorescence emission spectra of IKK FRET sensors. d) Western blot to demonstrate both the control and FRET sensor 2L are efficiently phosphorylated by IKK.